Structural Concrete
2001, **2**, No. ?
???, 1–11

Design of RC membrane elements

V. I. Carbone Politecnico of Turin, Italy

L. Giordano Politecnico of Turin, Italy

G. Mancini Politecnico of Turin, Italy

Over the last two decades, several theories for the design and verification of reinforced concrete (RC) membrane elements have been proposed on the basis of the experimental investigations conducted at a limited number of laboratories. In actual fact, in the definition of the behaviour of RC membrane elements, considerable difficulties of an experimental nature are compounded by the objective complexity of the physical model of reference. In this paper the theoretical models deemed most reliable are analysed, and those that can be used with greater ease for design purposes are identified and compared in terms of accuracy of the results provided, as determined on the basis of a significant number of tests performed at different laboratories.

Notation

General

E_c	elastic modulus of concrete
E_s	elastic modulus of steel
$\boldsymbol{f}'_c$	compressive strength of standard concrete cylinder (negative quantity)
$\boldsymbol{f}_{cr}$	stress in concrete at cracking
$\boldsymbol{f}_{c2\,max}$	compressive strength in 2-direction
$\boldsymbol{f}_{ysx}$, $\boldsymbol{f}_{ysy}$	yield stress of mild steel bars in *x* and *y* directions respectively
s_{rm}	spacing of cracks inclined at ϑ
s_{rmx0}, s_{rmy0}	average spacing of cracks perpendicular to the *x* and *y* reinforcements respectively
x, y	direction of longitudinal and transverse steel bars respectively
γ_{xy}	shear strain relative to *x*, *y* axes
ε_0	strain in concrete cylinder at peak stress (negative quantity)
ε_{cr}	strain in concrete at cracking
ε_x, ε_y	strain in *x* and *y* directions respectively
ρ_x, ρ_y	reinforcement ratio for reinforcing steel in *x* and *y* directions respectively
$\boldsymbol{\sigma}_{sx}$, $\boldsymbol{\sigma}_{xy}$	average stress in *x* and *y* reinforcements respectively
$\boldsymbol{\sigma}_{sxcr}$, $\boldsymbol{\sigma}_{sycr}$	stress in *x* and *y* reinforcements at crack location
$\boldsymbol{\sigma}_x$, $\boldsymbol{\sigma}_y$	stress applied to element in *x* and *y* directions respectively
$\boldsymbol{\tau}$	shear stress on element relative to *x*, *y* axes

Vecchio–Collins

a	maximum aggregate size
ε_1, ε_2	principal tensile and compressive strain in concrete (positive for tension)
ϑ	angle of inclination of principal strains to *x*-axis
ϑ_c	angle of inclination of principal stresses in concrete to *x*-axis
$\boldsymbol{\sigma}_{c1}$, $\boldsymbol{\sigma}_{c2}$	principal tensil and compressive (negative quantity) stress in concrete
$\boldsymbol{\sigma}_{ci}$	compressive stress on crack surface (positive quantity)
$\boldsymbol{\sigma}_{cx}$, $\boldsymbol{\sigma}_{cy}$	stress in concrete in *x* and *y* directions respectively
$\boldsymbol{\tau}_{ci}$	shear stress on crack surfaces
$\boldsymbol{\tau}_{ci\,max}$	maximum shear stress a crack of given width can resist
$\boldsymbol{\tau}_{cx}$, $\boldsymbol{\tau}_{cy}$	shear stress on *x* and *y* faces of concrete respectively
$\boldsymbol{\tau}_{cxy}$	shear stress on concrete relative to *x*, *y* axes
$\boldsymbol{\tau}_{sx}$, $\boldsymbol{\tau}_{sy}$	shear stress on *x* and *y* reinforcements respectively

Hsu

d, r	direction of principal compressive and tensile stress of concrete after cracking, respectively
E_p	elastic modulus of prestressing steel
E'_p	tangential modulus of Ramberg–Osgood curve at zero load
$\boldsymbol{f}_{pu}$	ultimate stength of prestressing steel
m	shape parameter

1, 2	direction of applied tensil and compressive principal stress respectively
α	angle of inclination of *d*-axis with respect to *x*-axis
α_2	fixed-angle of inclination of 2-axis with respect to *x*-axis
γ_{21}	average shear strain in 2,1-coordinate
γ_{21_0}	average shear strain in 2,1-coordinate at maximum shear stress τ_{21}^{m}
ε_d, ε_r	average principal strains in *d* and *r* directions respectively
ε_{dec}	decompression stress
ε_1, ε_2	average normal strains in 1- and 2-directions respectively
ζ	softening coefficient of concrete in compression
ρ_{xp}, ρ_{yp}	prestressed steel ratios in *x* and *y* directions respectively
$\boldsymbol{\sigma}_d$, $\boldsymbol{\sigma}_r$	principal stresses of concrete in *d* and *r* directions respectively
$\boldsymbol{\sigma}_1^c$, $\boldsymbol{\sigma}_2^c$	average normal stress of concrete in 1- and 2-directions respectively
$\boldsymbol{\sigma}_{sxp}$, $\boldsymbol{\sigma}_{syp}$	prestressed steel stress in *x* and *y* direction respectively
τ_{21}^c	average shear stress of concrete in 2,1-coordinate
τ_{21}^m	average maximum shear stress in 2,1-coordinate

Marti–Kaufmann

n, *t*	direction of principal tensile and compressive stress of concrete after cracking
ϑ	inclination of crack with respect to x-axis
$\boldsymbol{\sigma}_{cnr}$, $\boldsymbol{\sigma}_{ctr}$	concrete normal stress at crack in *n* and *t* directions respectively

Carbone–Giordano–Mancini

n_x, n_y	non-dimensional normal stress in *x* and *y* directions respectively ($\boldsymbol{\sigma}_x/\boldsymbol{f}_c'$, $\boldsymbol{\sigma}_y/\boldsymbol{f}_c'$)
v	non-dimensional shear stress in *x*, *y*-coordinate ($\tau/\boldsymbol{f}_c'$)
$\mathbf{v}_{max}$, $\mathbf{v}_{min}$	maximum and minimum non-dimensional shear stress in *x*, *y*-coordinate respectively
$\Delta\vartheta$	angle of deviation between the directions of principal compressive stresses in concrete in serviceability conditions and at failure
ϑ_e	angle of inclination of compressive stresses in concrete at serviceability conditions
ϑ_{pl}	angle of inclination of compressive stresses in concrete according to the assumption of perfectly plastic behaviour
ϑ_u	angle of inclination of compressive stresses in concrete at failure
ν	efficiency factor
$\boldsymbol{\sigma}_c$	oblique compressive stress in concrete
ω_x, ω_y	mechanical reinforcement ratios in *x* and *y* directions respectively ($\rho_x \boldsymbol{f}_{ysx}/\boldsymbol{f}_c'$, $\rho_y\, \boldsymbol{f}_{ysy}/\boldsymbol{f}_c'$)

Introduction

An analytical review of the studies conducted on reinforced concrete (RC) membrane elements over the last two decades makes it possible to enunciate four basic theoretical modelling proposals.

(1) The Modified Compression-Field Theory (MCFT) conceived by Vecchio and Collins (1986) on the basis of investigations performed at the University of Toronto.[1–4]
(2) The analysis of the behaviour of RC membranes through a rotating crack and a fixed angle crack approach, proposed by Hsu *et al.* (1991–1997), based on tests performed at the University of Houston.[5–10]
(3) The Cracked Membrane Model developed by Marti and Kaufmann (1999) on the basis of studies conducted at the ETH of Zurich.[11–13]
(4) The plastic model, based on a large number of tests, developed by Carbone, Giordano, Mancini (1999–2000) at the Politecnico of Turin.[14–16]

The different models are briefly illustrated and discussed below. Then, the models that can be used with ease for verification and design purposes are identified and compared in order to determine their reliability and working range, with reference to a large number of experimental results which are deemed reliable.

The Vecchio–Collins Model

The MCFT relies on the concept of smeared cracking—that is, it analyses the behaviour of a cracked element by considering a portion of it which is long enough to include several cracks and assuming that the effects of such cracks are evenly distributed over the entire portion. According to this model, which can be viewed, ultimately, as a macromodel, compatibility, equilibrium conditions and constitutive laws must be taken into account as follows.

Compatibility of strains

The concept of smeared cracking entails the need to assume a perfect bond between concrete and steel—that is, the composite, cracked material is treated as a continuum. If the three strain components, ε_x, ε_y, γ_{xy}, are known, *x* and *y* being the orthogonal directions of the reinforcement, then, through Mohr's circle, it is possible to determine the state of strain along any direction. In particular, we find

$$\gamma_{xy} = \frac{2(\varepsilon_x - \varepsilon_2)}{\tan\vartheta} \tag{1}$$

$$\varepsilon_x + \varepsilon_y = \varepsilon_1 + \varepsilon_2 \tag{2}$$

$$\tan^2\vartheta = \frac{(\varepsilon_x - \varepsilon_2)}{(\varepsilon_y - \varepsilon_2)} = \frac{(\varepsilon_1 - \varepsilon_y)}{(\varepsilon_1 - \varepsilon_x)} = \frac{(\varepsilon_1 - \varepsilon_y)}{(\varepsilon_y - \varepsilon_2)} = \frac{(\varepsilon_x - \varepsilon_2)}{(\varepsilon_1 - \varepsilon_x)} \tag{3}$$

where ε_1 and ε_2 are the principal strains and ϑ identifies their direction.

Equilibrium conditions

Equilibrium conditions can be set with reference to the free body diagram shown in Figure 1

$$\boldsymbol{\sigma}_x = \boldsymbol{\sigma}_{cx} + \rho_x \boldsymbol{\sigma}_{sx} \tag{4}$$

$$\boldsymbol{\sigma}_y = \boldsymbol{\sigma}_{cy} + \rho_y \boldsymbol{\sigma}_{sy} \tag{5}$$

$$\boldsymbol{\tau} = \boldsymbol{\tau}_{cx} + \rho_x \boldsymbol{\tau}_{sx} \tag{6}$$

$$\boldsymbol{\tau} = \boldsymbol{\tau}_{cy} + \rho_y \boldsymbol{\tau}_{sy} \tag{7}$$

and, having set $\tau_{cx} = \tau_{cy} = \tau_{cxy}$, stress conditions can be defined

FIRST PROOFS CJ I:/Thomas Telford/Sc/sc-39.3d Page: 2 SC 39 Keyword

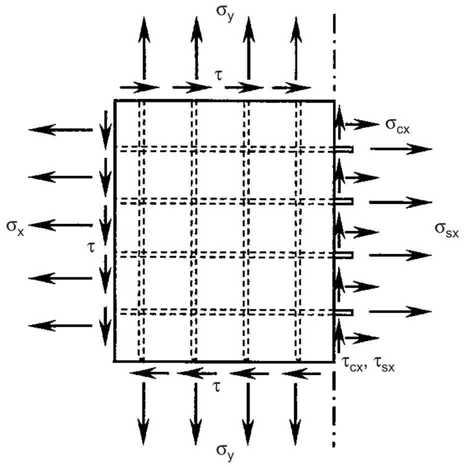

Fig. 1 Free-body diagram of sectioned element

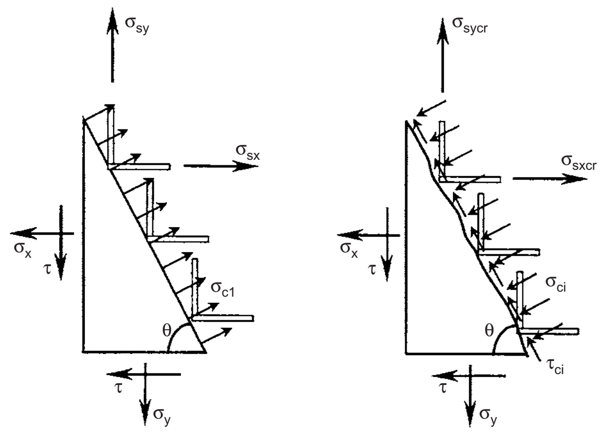

Fig. 2 Comparison of local stresses at a crack with calculated average stresses

when $\boldsymbol{\sigma}_{cx}$, $\boldsymbol{\sigma}_{cy}$ and τ_{cxy} have been determined. In this case too, with the aid of Mohr's circle, we can write

$$\boldsymbol{\sigma}_{cx} = \frac{\boldsymbol{\sigma}_{c1} - \tau_{cxy}}{\tan\vartheta_c} \tag{8}$$

$$\boldsymbol{\sigma}_{cy} = \boldsymbol{\sigma}_{c1} - \tau_{cxy}\tan\vartheta_c \tag{9}$$

$$\boldsymbol{\sigma}_{c2} = \boldsymbol{\sigma}_{c1} - \tau_{cxy}(\tan\vartheta_c + \cot\vartheta_c) \tag{10}$$

where $\boldsymbol{\sigma}_{c1}$ and $\boldsymbol{\sigma}_{c2}$ are the principal stresses and ϑ_c, identifies their direction.

Constitutive laws

Though they are derived from the laws of the individual materials, constitutive laws must be defined with reference to the mean composite material corresponding to the assumption of smeared cracking. For the behaviour of steel, a bilinear law is assumed, with yield strength as its limit value; it is also assumed that the reinforcement is able to carry only the longitudinal stress, and hence $\tau_{sx} = \tau_{sy} = 0$. The constitutive law for concrete in compression, worked out directly from test results (30 panels tested in Toronto), highlights the reduction in strength in the principal direction of compression brought about by the tensile stresses applied orthogonally to the latter. The proposed law is as follows

$$\boldsymbol{\sigma}_{c2} = \boldsymbol{f}_{c2\,max}\left[2\left(\frac{\varepsilon_2}{\varepsilon_0}\right) - \left(\frac{\varepsilon_2}{\varepsilon_0}\right)^2\right] \tag{11}$$

where

$$\frac{\boldsymbol{f}_{c2\,max}}{\boldsymbol{f}'_c} = \frac{1}{0{\cdot}8 - 0{\cdot}34(\varepsilon_2/\varepsilon_0)} \leq 1 \tag{12}$$

The constitutive law proposed for concrete in tension is

$$\boldsymbol{\sigma}_{c1} = E_c\varepsilon_1 \qquad \text{for } \varepsilon_1 \leq \varepsilon_{cr} \tag{13}$$

$$\boldsymbol{\sigma}_{c1} = \frac{\boldsymbol{f}_{cr}}{1 + \sqrt{200\varepsilon_1}} \qquad \text{for } \varepsilon_1 > \varepsilon_{cr} \tag{14}$$

Furthermore, it is assumed that the principal directions of strain and stress coincide, even though the tests have revealed angular differences of up to $\pm 10^\circ$ between ϑ and ϑ_c.

A study of the local behaviour of the crack is conducted by comparing stress conditions in the plane of the crack, which is taken to be the principal plane, based on the assumption of mean behaviour, with the real forces acting on the same plane (Figure 2). Since the two stress systems correspond to the same actions applied we can write

$$\rho_x\boldsymbol{\sigma}_{sx}\sin\vartheta + \boldsymbol{\sigma}_{c1}\sin\vartheta = \rho_x\boldsymbol{\sigma}_{sxcr}\sin\vartheta - \boldsymbol{\sigma}_{ci}\sin\vartheta - \tau_{ci}\cos\vartheta \tag{15}$$

$$\rho_y\boldsymbol{\sigma}_{sy}\cos\vartheta + \boldsymbol{\sigma}_{c1}\cos\vartheta = \rho_y\boldsymbol{\sigma}_{sycr}\cos\vartheta - \boldsymbol{\sigma}_{ci}\cos\vartheta - \tau_{ci}\sin\vartheta \tag{16}$$

which means that equilibrium conditions can be reached without any actions being transmitted across the crack only if

$$\boldsymbol{\sigma}_{sy}(\boldsymbol{\sigma}_{sycr} - \boldsymbol{\sigma}_{sy}) = \rho_x(\boldsymbol{\sigma}_{sxcr} - \boldsymbol{\sigma}_{sx}) = \boldsymbol{\sigma}_{c1} \tag{17}$$

The constitutive law for the actions transferred across the crack is proposed on the basis of the tests performed by Walraven[17]

$$\tau_{ci} = 0{\cdot}18\tau_{ci\,max} + 1{\cdot}64\boldsymbol{\sigma}_{ci} - 0{\cdot}82\frac{\boldsymbol{\sigma}_{ci}^2}{\tau_{ci\,max}} \tag{18}$$

where

$$\tau_{ci\,max} = \frac{\sqrt{-\boldsymbol{f}'_c}}{0{\cdot}31 + 24w/(a+16)} \tag{19}$$

where a represents maximum aggregate diameter and w is the mean width of the crack, $w = \varepsilon_1 s_{rm}$, where

$$s_{rm} = \frac{1}{\dfrac{\sin\vartheta}{s_{rmx0}} + \dfrac{\cos\vartheta}{s_{rmy0}}} \tag{20}$$

where s_{rmx0} and s_{rmy0} stand for the spacing of the cracks in the x and y directions, respectively.

Overview

The complex systems of non-linear equations governing the response of the element must be solved through an iterative process, according to the instructions supplied by the Vecchio and Collins. Although the computation process involved is too burdensome to be used in today's design practice, the solutions obtained are appreciably accurate. This model must be given credit for having rationalised the approach to the definition of the mechanical behaviour of RC membrane elements, and having pointed out the marked reduction in strength that takes place in the compressive stress fields of the concrete when appreciable tensile stress fields are active in a direction orthogonal to them.

FIRST PROOFS CJ I:/Thomas Telford/Sc/sc-39.3d Page: 3 SC 39 Keyword

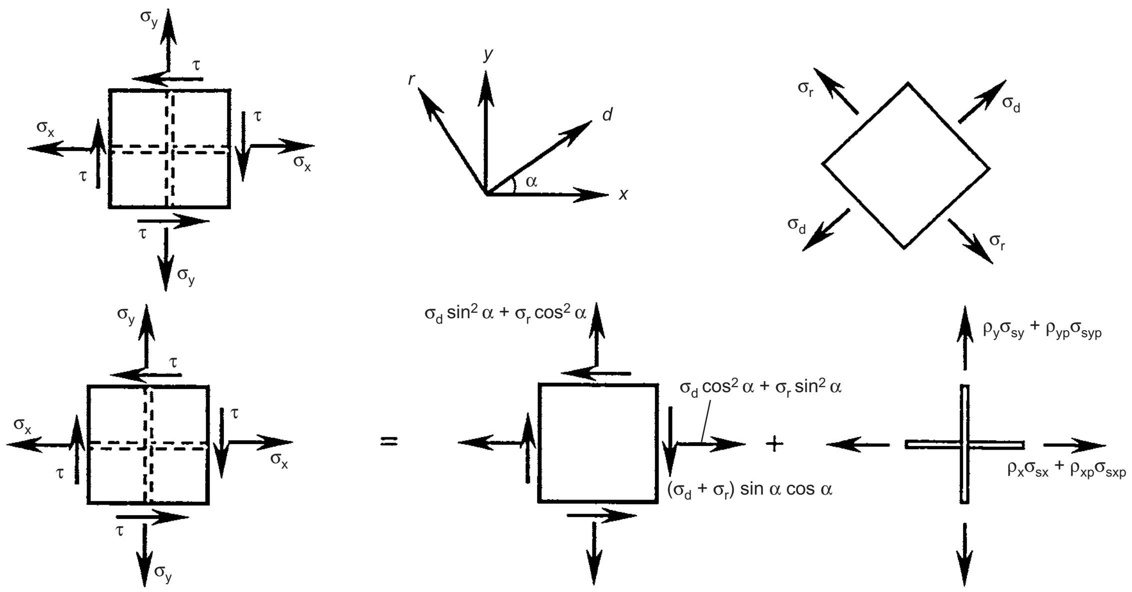

Fig. 3 Stress conditions in reinforced concrete membrane element

Hsu's models

Rotating crack type model

The first model proposed by Hsu, of the rotating crack type, is based on the assumption that the opening of the cracks is followed by the formation of a system of struts: compression struts of concrete, and tension struts of steel. This system is assumed to be arranged at an angle α relative to the x, y directions of the reinforcement, and it is also assumed that the same angle, α, identifies the principal directions of the stresses and strains in the concrete (which are therefore assumed to coincide). Furthermore, it is assumed that the reinforcement can only carry longitudinal stresses.

Equilibrium equations. With reference to Figure 3, it proves easy to write the following three equilibrium conditions

$$\boldsymbol{\sigma}_{\mathrm{x}} = \boldsymbol{\sigma}_{\mathrm{d}} \cos^2\alpha + \boldsymbol{\sigma}_{\mathrm{r}} \sin^2\alpha + \rho_{\mathrm{x}}\boldsymbol{\sigma}_{\mathrm{sx}} + \rho_{\mathrm{xp}}\boldsymbol{\sigma}_{\mathrm{sxp}} \tag{21}$$

$$\boldsymbol{\sigma}_{\mathrm{y}} = \boldsymbol{\sigma}_{\mathrm{d}} \sin^2\alpha + \boldsymbol{\sigma}_{\mathrm{r}} \cos^2\alpha + \rho_{\mathrm{y}}\boldsymbol{\sigma}_{\mathrm{sy}} + \rho_{\mathrm{yp}}\boldsymbol{\sigma}_{\mathrm{syp}} \tag{22}$$

$$\boldsymbol{\tau} = (-\boldsymbol{\sigma}_{\mathrm{d}} + \boldsymbol{\sigma}_{\mathrm{r}}) \sin\alpha\cos\alpha \tag{23}$$

Compatibility equations. Always working in terms of smeared cracking, and hence of a continuum equivalent to the cracked membrane element, we can write

$$\varepsilon_{\mathrm{x}} = \varepsilon_{\mathrm{d}} \cos^2\alpha + \varepsilon_{\mathrm{r}} \sin^2\alpha \tag{24}$$

$$\varepsilon_{\mathrm{y}} = \varepsilon_{\mathrm{d}} \sin^2\alpha + \varepsilon_{\mathrm{r}} \cos^2\alpha \tag{25}$$

$$\gamma_{\mathrm{xy}} = 2(-\varepsilon_{\mathrm{d}} + \varepsilon_{\mathrm{r}}) \sin\alpha\cos\alpha \tag{26}$$

To solve equations (21) to (26) it is necessary to introduce six corresponding constitutive relationships for the materials, two of which are for concrete in directions d and r and two are for each of the two types of steel, in directions x and y.

Constitutive laws. The behaviour of concrete in compression is according to the proposal by Vecchio and Collins described above

$$\boldsymbol{\sigma}_{\mathrm{d}} = \zeta \boldsymbol{f}'_{\mathrm{c}}\left[2\left(\frac{\varepsilon_{\mathrm{d}}}{\zeta\varepsilon_0}\right) - \left(\frac{\varepsilon_{\mathrm{d}}}{\zeta\varepsilon_0}\right)^2\right] \quad \text{for } \varepsilon_{\mathrm{d}}/\zeta\varepsilon_0 \leq 1 \tag{27}$$

$$\boldsymbol{\sigma}_{\mathrm{d}} = \zeta \boldsymbol{f}'_{\mathrm{c}}\left[1 - \left(\frac{\varepsilon_{\mathrm{d}}/\zeta\varepsilon_0 - 1}{2\zeta - 1}\right)^2\right] \quad \text{for } \varepsilon_{\mathrm{d}}/\zeta\varepsilon_0 > 1 \tag{28}$$

where the softening coefficient ($0 < \zeta < 1$) assumes the following form

$$\zeta = \frac{1}{\sqrt{0{\cdot}7 - (\varepsilon_{\mathrm{r}}/\varepsilon_{\mathrm{d}})}} \tag{29}$$

For the concrete in tension the following expressions are adopted instead

$$\boldsymbol{\sigma}_{\mathrm{r}} = E_{\mathrm{c}}\varepsilon_{\mathrm{r}} \quad \text{for } \varepsilon_{\mathrm{r}} \leq \varepsilon_{\mathrm{cr}} \tag{30}$$

$$\boldsymbol{\sigma}_{\mathrm{r}} = \frac{\boldsymbol{f}_{\mathrm{cr}}}{1 + \sqrt{\dfrac{\varepsilon_{\mathrm{r}} - \varepsilon_{\mathrm{cr}}}{0{\cdot}005}}} \quad \text{for } \varepsilon_{\mathrm{r}} > \varepsilon_{\mathrm{cr}} \tag{31}$$

For ordinary steel the law adopted is an elasto-plastic bilinear law whose limit value corresponds to yield strength. For prestressing steel, account taken of the pre-elongation associated with prestressing and its possible increase up to concrete decompression, the proposed constitutive law is

$$\boldsymbol{\sigma}_{\mathrm{sp}} = E_{\mathrm{p}}(\varepsilon_{\mathrm{dec}} + \varepsilon) \quad \text{for } \boldsymbol{\sigma}_{\mathrm{sp}} \leq 0{\cdot}7\,\boldsymbol{f}_{\mathrm{pu}} \tag{32a}$$

$$\boldsymbol{\sigma}_{\mathrm{sp}} = \frac{E'_{\mathrm{p}}(\varepsilon_{\mathrm{dec}} + \varepsilon)}{\left\{1 + \left[\dfrac{E'_{\mathrm{p}}(\varepsilon_{\mathrm{dec}} + \varepsilon)}{\boldsymbol{f}_{\mathrm{pu}}}\right]^{\mathrm{m}}\right\}^{1/\mathrm{m}}} \quad \text{for } \boldsymbol{\sigma}_{\mathrm{sp}} > 0{\cdot}7\,\boldsymbol{f}_{\mathrm{pu}} \tag{32b}$$

In this manner we get a system consisting of 13 non-linear equations in 16 unknowns, of which nine are stress components and six are strain components. If the three external stress components, $\boldsymbol{\sigma}_{\mathrm{x}}$, $\boldsymbol{\sigma}_{\mathrm{y}}$, $\boldsymbol{\tau}$, are assumed to be known, the system can be solved by means of an iterative procedure suggested by Hsu.

At a later stage, Hsu points out that the assumption of angle α and angle α_2 being the same (α and α_2 identifying the inclination of the principal axes of the stresses in the concrete struts after the opening of the cracks and the inclination of the principal axes of the stresses applied to the element, respectively) applies only if the values of smeared strength of steel in directions x and y also coincide. If they do not, when the cracks are formed, equilibrium

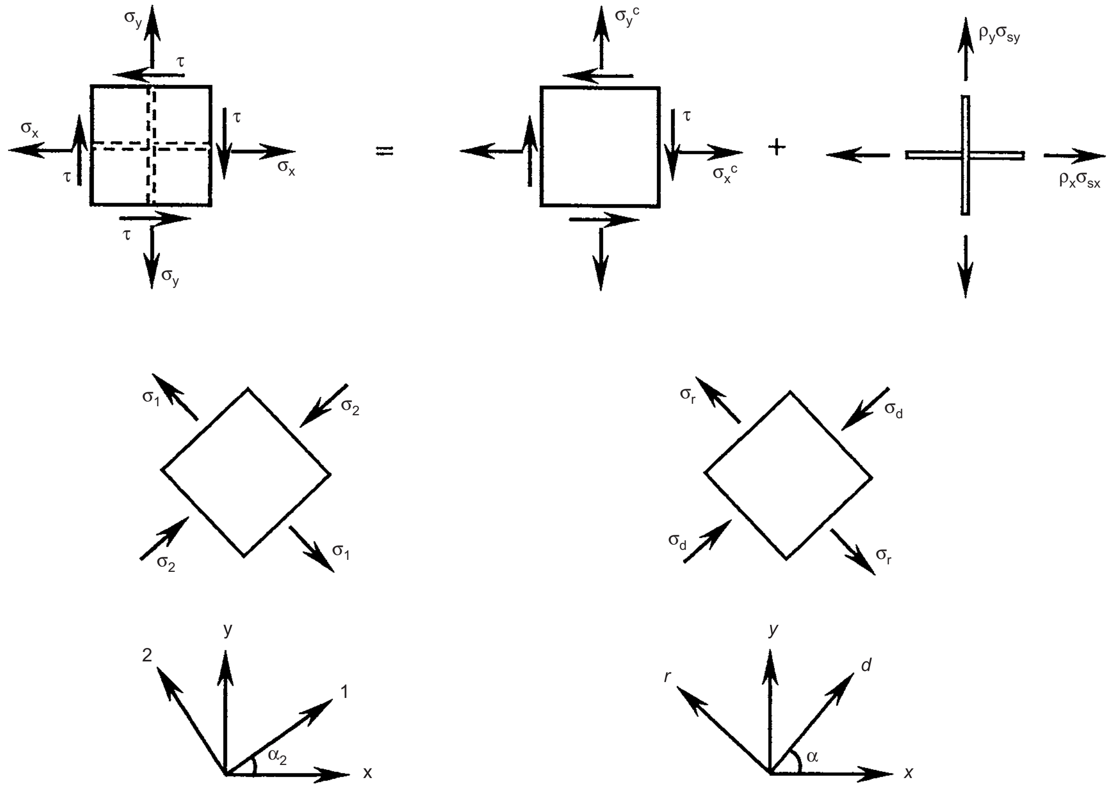

Fig. 4 Stress conditions in reinforced concrete

conditions can be reached only if angle α differs from angle α_2 by a quantity β (Figure 4). Obviously, equilibrium and congruence conditions remain unchanged and the constitutive laws of the materials are only partly modified. In particular, for concrete in compression a different softening coefficient is proposed

$$\zeta = \frac{0{\cdot}9}{\sqrt{1+400\varepsilon_r}} \tag{33}$$

while for the concrete in tension the constitutive law becomes

$$\boldsymbol{\sigma}_r = E_c\boldsymbol{\varepsilon}_r \qquad \text{for } \varepsilon_r \leq 0{\cdot}00008 \tag{34}$$

$$\boldsymbol{\sigma}_r = \boldsymbol{f}_{cr}\left(\frac{0{\cdot}00008}{\varepsilon_r}\right)^{0{\cdot}4} \qquad \text{for } \varepsilon_r > 0{\cdot}00008 \tag{35}$$

Another phenomenon which is observed in the tests is the kinking of the steel bars—that is, an apparent reduction in their longitudinal strength due to the effect of tension combined with the dowel effect triggered by the transverse behaviour along the crack. To be able to take this phenomenon into account, the constitutive law of steel is modified by introducing an apparent yield stress.

In any case we return to a system consisting of 13 non-linear equations. Another important observation, arising from a systematic application of the proposed model to a set of 13 panels subjected to tests, it that the physical model based on the rotation of the cracking angle cannot describe the behaviour of RC membrane elements having a II mechanical reinforcement ratio, in either direction, which is not within the range

$$0{\cdot}4 \leq \frac{\rho_y \boldsymbol{f}_{ysy}}{\rho_x \boldsymbol{f}_{ysx}} \leq 2{\cdot}5 \tag{36}$$

which amounts to saying that the model is valid only if angle α is within the range

$$33^\circ \leq \alpha \leq 57^\circ \tag{37}$$

If it is not, it becomes necessary to resort to the third model proposed by Hsu, which consists of a softened truss model characterised by a fixed cracking angle.

Fixed crack type model

The equations characterising the behaviour of this model can be written with reference to Figures 4 and 5. In particular, based on equilibrium considerations, we get

$$\boldsymbol{\sigma}_x = \boldsymbol{\sigma}_2^c \cos^2\alpha_2 + \boldsymbol{\sigma}_1^c \sin^2\alpha_2 + \boldsymbol{\tau}_{21}^c 2\sin\alpha_2\cos\alpha_2 + \rho_x\boldsymbol{\sigma}_{sx} \tag{38}$$

$$\boldsymbol{\sigma}_y = \boldsymbol{\sigma}_2^c \sin^2\alpha_2 + \boldsymbol{\sigma}_1^c \cos^2\alpha_2 + \boldsymbol{\tau}_{21}^c 2\sin\alpha_2\cos\alpha_2 + \rho_y\boldsymbol{\sigma}_{sy} \tag{39}$$

$$\boldsymbol{\tau} = (-\boldsymbol{\sigma}_2^c + \boldsymbol{\sigma}_1^c)\sin\alpha_2\cos\alpha_2 + \boldsymbol{\tau}_{21}^c(\cos^2\alpha_2 - \sin^2\alpha_2) \tag{40}$$

In these equations, $\boldsymbol{\tau}_{21}^c$ stands for mean shear transferred along the crack, and can be represented through the following relationship, of an experimental nature

$$\boldsymbol{\tau}_{21}^c = \boldsymbol{\tau}_{21}^m\left[1-\left(1-\frac{\gamma_{21}}{\gamma_{21_0}}\right)^6\right] \tag{41}$$

For the compatibility equations, always with reference to a continuum equivalent to smeared cracking, this gives

$$\varepsilon_x = \varepsilon_2\cos^2\alpha_2 + \varepsilon_1\sin^2\alpha_2 + \frac{\gamma_{21}}{2}2\sin\alpha_2\cos\alpha_2 \tag{42}$$

$$\varepsilon_y = \varepsilon_2\sin^2\alpha_2 + \varepsilon_1\cos^2\alpha_2 + \frac{\gamma_{21}}{2}2\sin\alpha_2\cos\alpha_2 \tag{43}$$

$$\frac{\gamma_{xy}}{2} = (-\varepsilon_2+\varepsilon_1)\sin\alpha_2\cos\alpha_1 + \frac{\gamma_{21}}{2}(\cos^2\alpha_2 - \sin^2\alpha_2) \tag{44}$$

As to the constitutive laws, for the concrete in compression, a new softening coefficient is proposed

FIRST PROOFS CJ I:/Thomas Telford/Sc/sc-39.3d Page: 5 SC 39 Keyword

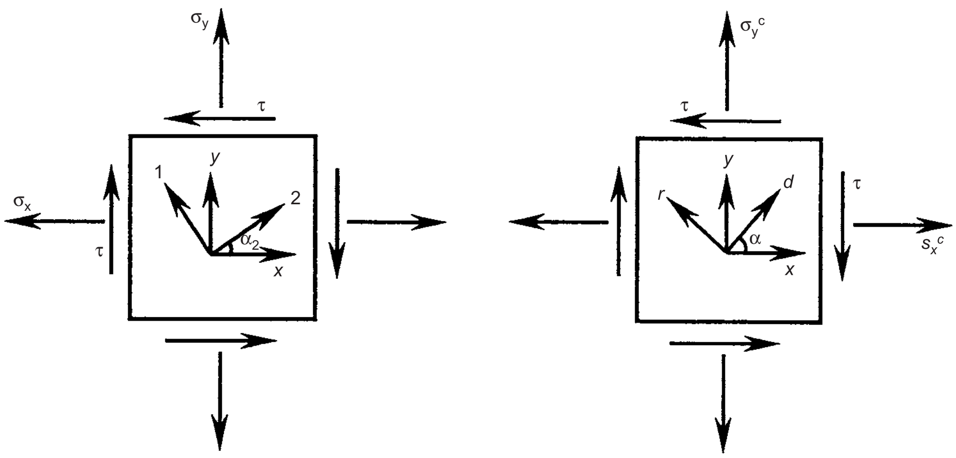

Fig. 5 Crack directions in fixed- and rotating-angle models

$$\zeta = \frac{5{\cdot}8}{\sqrt{f_c'}} \frac{1}{\sqrt{1 + \frac{400}{\eta}\varepsilon_1}} \tag{45}$$

where

$$\eta = \frac{\rho_y \boldsymbol{f}_{ysy} - \boldsymbol{\sigma}_y}{\rho_x \boldsymbol{f}_{ysx} - \boldsymbol{\sigma}_x} \tag{46}$$

Ultimately, we get a system consisting of twelve non-linear equations to be solved by means of an ad hoc iterative process. In actual fact, this model represents a considerable improvement over the earlier models in that it is more reliable and makes it possible to extend the validity of the procedure to the instances in which coefficient η is in the following range

$$0{\cdot}2 \le \eta \le 5 \tag{47}$$

that is, within a range twice as big as in the previous case.

Overview

All in all, the different models proposed by Hsu and his collaborators can be rated as a valuable approach to the behaviour of RC membranes, but the resolution processes involved are too complex to be used widely by practising designers.

The Marti–Kaufmann Model

The model proposed by Marti and Kaufmann combines the basic concepts of MCFT with the tension chord model developed by the authors. In actual practice, the spacing of the cracks and the tensile stresses between the cracks are determined with the aid of constitutive laws for bond and equilibrium equations, which are formulated in terms of stresses at the cracks, instead of in terms of mean stresses between cracks (smeared cracking). The faces of the cracks are assumed to be stress-free, able to rotate and arranged orthogonally to the principal direction of the principal strains.

With reference to Figure 6 we can write the following equilibrium equations

$$\boldsymbol{\sigma}_x = \rho_x \boldsymbol{\sigma}_{sxcr} + \boldsymbol{\sigma}_{cnr} \sin^2 \vartheta_r + \boldsymbol{\sigma}_{ctr} \cos^2 \vartheta_r - \boldsymbol{\tau}_{ctnr} \sin(2\vartheta_r) \tag{48}$$

$$\boldsymbol{\sigma}_y = \rho_y \boldsymbol{\sigma}_{sycr} + \boldsymbol{\sigma}_{cnr} \cos^2 \vartheta_r + \boldsymbol{\sigma}_{ctr} \sin^2 \vartheta_r + \boldsymbol{\tau}_{ctnr} \sin(2\vartheta_r) \tag{49}$$

$$\boldsymbol{\tau} = (\boldsymbol{\sigma}_{cnr} - \boldsymbol{\sigma}_{ctr}) \sin \vartheta_r \cos \vartheta_r - \boldsymbol{\tau}_{ctnr} \cos(2\vartheta_r) \tag{50}$$

Fig. 6 Cracked membrane—general considerations

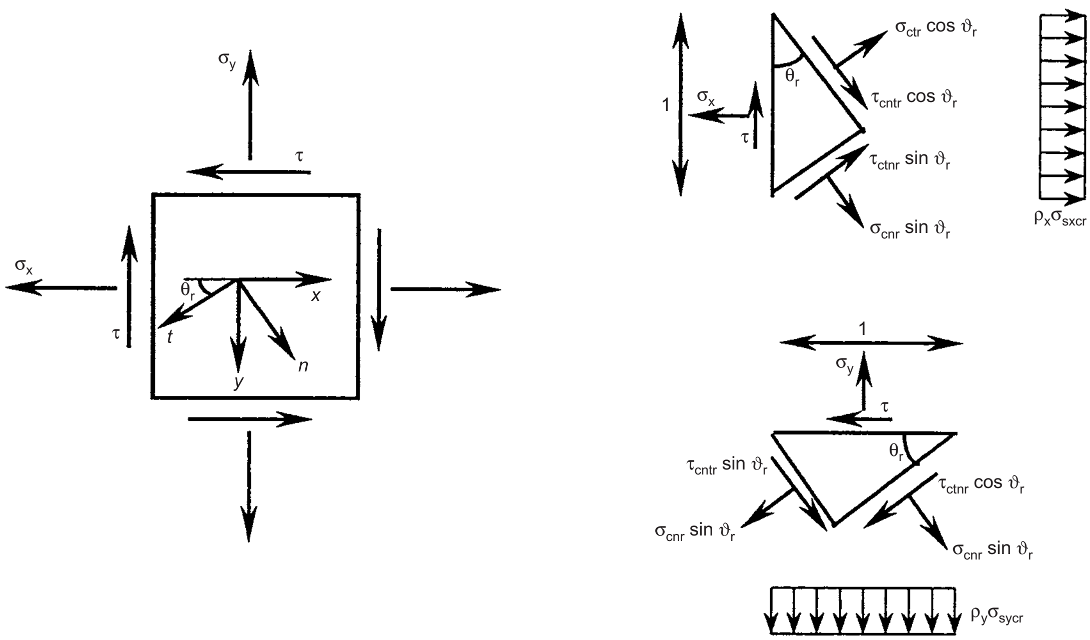

FIRST PROOFS CJ I:/Thomas Telford/Sc/sc-39.3d Page: 6 SC 39 Keyword

in which, by virtue of the foregoing assumptions, we must set $\sigma_{cnr} = \tau_{ctnr} = 0$.

For stress in the concrete compressive field a parabolic expression is adopted, of the following form

$$\sigma_{ctr} = \frac{f_{c2\,max}(\varepsilon_2^2 + 2\varepsilon_2\varepsilon_0)}{\varepsilon_0^2} \tag{51}$$

$$f_{c2\,max} = \frac{(f'_c)^{2/3}}{0{\cdot}4 + 30\varepsilon_1} \le f'_c \tag{52}$$

$\varepsilon_1/\varepsilon_2$ being the principal strains and ε_{c0} the peak strain of the constitutive law. The mean spacing of the cracks can be obtained through Vecchio and Collins' expression

$$s_{rm} = \frac{1}{\dfrac{\sin\vartheta_r}{s_{rmx0}} + \dfrac{\cos\vartheta}{s_{rmz0}}} \tag{53}$$

Now, considering ε_x, ε_y, ε_2 as unknowns and observing that $\varepsilon_1 = \varepsilon_x + \varepsilon_y - \varepsilon_2$ and $\tan^2\vartheta = (\varepsilon_x - \varepsilon_2)/(\varepsilon_y - \varepsilon_2)$, all the quantities appearing in equations (48) to (50) can be expressed as a function of the unknown strain components; σ_{sxcr} and σ_{sycr}, in fact, are derived from the constitutive equations of the tension chord model, and σ_{ctr}, from equations (52) and (53). Hence, for each set of stresses, $\sigma_x/\sigma_y/\tau$, it is possible to work out the corresponding set of strains, $\varepsilon_x/\varepsilon_y/\varepsilon_2$, by means of an iterative procedure.

If it is assumed that the tensile stresses acting between, two cracks vary linearly from zero to f_{cr} over half the distance between the cracks, we get the following equation

$$\begin{aligned}\tan^2\vartheta_r\rho_x(1+n\rho_y) + \tan\vartheta_r\rho_x\left[\frac{\sigma_y}{\tau} - \frac{f_{cr}}{2\tau}(1+n\rho_y)\right] \\ = \cot^2\vartheta_r\rho_y(1+n\rho_x) \\ + \cot\vartheta_r\rho_y\left[\frac{\sigma_x}{\tau} - \frac{f_{cr}}{2\tau}(1+n\rho_x)\right]\end{aligned} \tag{54}$$

which, under the assumption of $f_{cr} = 0$, coincides with the typical equation of the compression field approach worked out by Baumann[18] in 1972

$$\tan^2\vartheta_r\rho_r(1+n\rho_y) + \tan\vartheta_r\rho_x\frac{\sigma_y}{\tau} = \cot^2\vartheta_r\rho_y(1+n\rho_x) + \cot\vartheta_r\rho_y\frac{\sigma_x}{\tau} \tag{55}$$

At this point, by introducing the assumptions of limit analysis we can work out the following three equations

$$\tau^2 - (\rho_x f_{ysx} - \sigma_x)(\rho_y f_{ysy} - \sigma_y) = 0 \tag{56}$$

$$\tau^2 - (f_c - \rho_{x,y} f_{ysx,y} + \sigma_{x,y})(\rho_{x,y} f_{ysx,y} - \sigma_{x,y}) = 0 \tag{57}$$

$$\tau^2 - \frac{f_c^2}{4} = 0 \tag{58}$$

Introducing the following expression for the compressive strength of concrete

$$f_{c2\,max} = 1{\cdot}7 f_c'^{(2/3)} \tag{59}$$

and assuming that the strain in steel, in the direction in which it does not reach the yield point, is $0{\cdot}8\ f_{ys}/E_s$ at the ultimate limit state, the equations describing the limit surface become

$$\tau^2 = (\rho_x f_{ysx} - \sigma_x)(\rho_y f_{ysy} - \sigma_y) \tag{60}$$

$$\tau^2 = (\rho_{x,y} f_{ysx,y} - \sigma_{x,y})^2\left(\sqrt{2 + \frac{25}{3}\frac{f_c'^{(2/3)}}{\rho_{x,y} f_{ysx,y} - \sigma_{x,y}}} - \frac{29}{12}\right) \tag{61}$$

$$\tau^2 = \left(\frac{25}{29} f_c'^{(2/3)}\right)^2 \tag{62}$$

Figure 7 illustrates the limit surface obtained with the cracked membrane model and the design equations in their simplified form (equations (60)–(62)).

It can be concluded that the model developed by Marti and Kaufmann, by introducing simplifications that make for improved safety, represents a valid instrument for the design and checking of RC membrane elements, with a degree of computational complexity that can be rated as acceptable for current design purposes.

Model by Carbone, Giordano and Mancini

The model proposed by Carbone, Giordano and Mancini is based on the assumption that the strength of concrete subjected to biaxial stresses is correlated to the angular deviation $\Delta\vartheta$ between angle ϑ_{el}, which identifies the principal compressive stresses in uncracked state, incipient cracking conditions, and angle ϑ_u,

Fig. 7 Failure surfaces: (a) cracked membrane; and (b) design equations

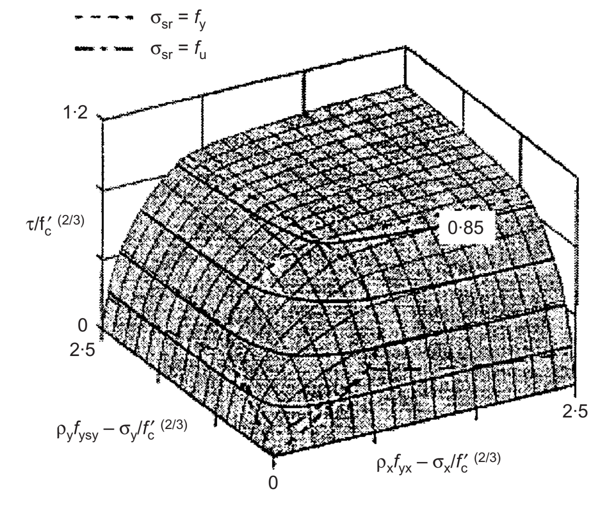

(a)

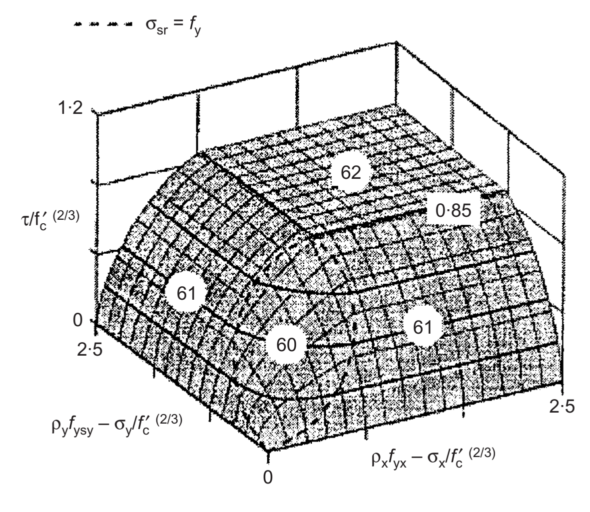

(b)

FIRST PROOFS CJ I:/Thomas Telford/Sc/sc-39.3d Page: 7 SC 39 Keyword

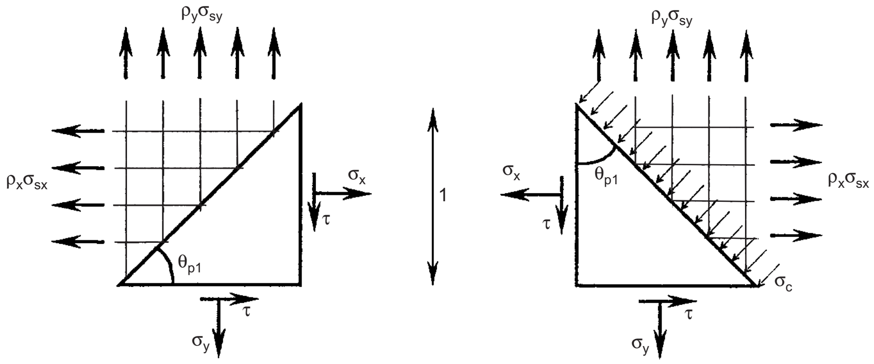

Fig. 8 Plastic equilibrium condition

which identifies the inclination of the oblique stress field that is present in concrete when the ultimate limit state is reached. With increasing $\Delta\vartheta$, concrete damage increases progressively and concrete strength is reduced accordingly.

Initially, angle ϑ_u is evaluated numerically by reproducing, with the aid of ADINA, a significant number of the tests described by Vecchio, Collins and Belarbi, and Hsu in which failure was clearly seen to occur in the concrete. To this end, the concrete is described by means of a constitutive law defined as a function of the initial strain modulus, the tensile strength and the compressive strength as determined in a uniaxial test and the corresponding strains. In actual practice, with reference to the method proposed by Von Grabe and Tworuschka,[19] a constitutive law corresponding, at least in the ascending branch, to Sargin's law is described. Furthermore, the model uses the failure surface proposed by Kotsovos[20] on the basis of extensive testing conducted at the Imperial College, London.

For steel, an elasto-plastic constitutive law is adopted, with a work-hardening modulus corresponding to 1% of the elastic modulus.

Based on the results of the numerical calculations, an interpolating law of the type

$$\upsilon = \frac{\boldsymbol{\sigma}_c}{|\boldsymbol{f}_c'|} = 0{\cdot}55 - 0{\cdot}12 \ln|\Delta\vartheta| \qquad (63)$$

is proposed for ultimate concrete strength.

A further step consists of demonstrating that angle ϑ_u, can be viewed as coinciding, with an acceptable degree of approximation, with angle ϑ_{pl}, which identifies the inclination of the field of oblique stresses in concrete according to the assumption of perfectly plastic behaviour. According to this assumption, the effect of the actions exchanged between the surfaces of the crack is a variation in the angle of the oblique compressive stress field, which can be evaluated, under the assumption of smeared cracking, with respect to the angle of the crack. With reference to Figure 8 it then becomes possible to impose the following equilibrium conditions

$$\boldsymbol{\sigma}_x + \boldsymbol{\tau}\cot\vartheta_{pl} - \boldsymbol{\sigma}_{sx}\rho_x = 0 \qquad (64)$$

$$\boldsymbol{\tau} + \boldsymbol{\sigma}_x\cot\vartheta_{pl} - \boldsymbol{\sigma}_{sy}\rho_y\cot\vartheta_{pl} = 0 \qquad (65)$$

$$\boldsymbol{\tau}\tan\vartheta_{pl} - \boldsymbol{\sigma}_x + \boldsymbol{\sigma}_{sx}\rho_x - \boldsymbol{\sigma}_c = 0 \qquad (66)$$

$$\boldsymbol{\tau} - \boldsymbol{\sigma}_y\tan\vartheta_{pl} + \boldsymbol{\sigma}_{sy}\rho_y\tan\vartheta_{pl} - \boldsymbol{\sigma}_c\tan\vartheta_{pl} = 0 \qquad (67)$$

By making the necessary substitution and introducing the strength criterion given by expression (63), we get an equation in one unknown, ϑ_{pl}

$$\frac{\boldsymbol{\tau}}{|\boldsymbol{f}_c'|}(\tan\vartheta_{pl} + \cot\vartheta_{pl}) - [0{\cdot}55 - 0{\cdot}12\ln|\vartheta_{pl} - \vartheta_{el}|] = 0 \qquad (68)$$

By introducing the limit strength conditions for the materials ($-\boldsymbol{f}_{ysx} \leq \boldsymbol{\sigma}_{sx} \leq \boldsymbol{f}_{ysx}$, $-\boldsymbol{f}_{ysy} \leq \boldsymbol{\sigma}_{sy} \leq \boldsymbol{f}_{ysy}$, $\boldsymbol{\sigma}_c \leq \nu|\boldsymbol{f}_c'|$) and working in dimensional terms, we may now work out the following system of inequalities

$$\boldsymbol{v} \geq -(\omega_x + n_x)\tan\vartheta_{pl} \qquad (69)$$

$$\boldsymbol{v} \leq (\omega_x - n_x)\tan\vartheta_{pl} \qquad (70)$$

$$\boldsymbol{v} \geq (-\omega_y + n_y)\cot\vartheta_{pl} \qquad (71)$$

$$\boldsymbol{v} \leq (\omega_y - n_y)\cot\vartheta_{pl} \qquad (72)$$

$$\boldsymbol{v} \leq \nu\sin\vartheta_{pl}\cos\vartheta_{pl} \qquad (73)$$

By solving this system it proves possible to identify a range of values of $\boldsymbol{v}$ corresponding to the strength conditions of the element, as a function of ω_x, ω_y, n_x, n_y, $\Delta\vartheta$. Figure 9 illustrates the relationship $\boldsymbol{v} = \boldsymbol{f}(\vartheta_{pl})$, for specific values of $\omega_x = 0{\cdot}16/\omega_y = 0{\cdot}06/$

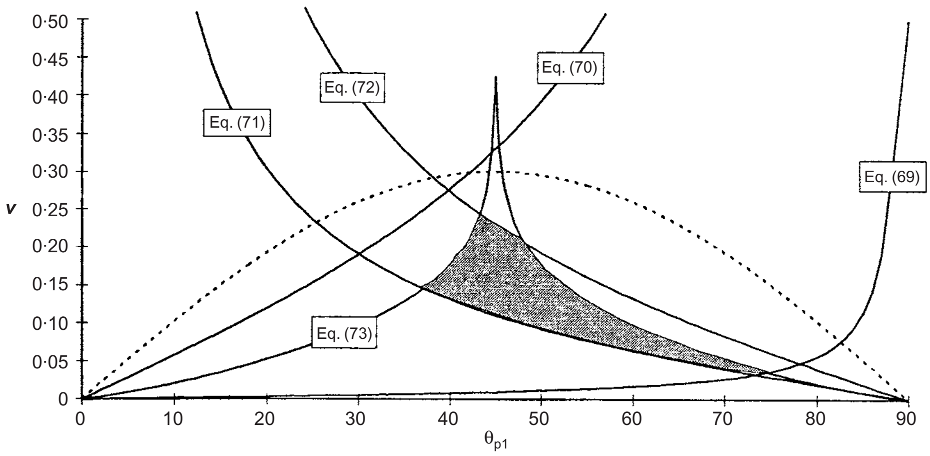

Fig. 9 Graphical solution of disequation system (69) to (73)

FIRST PROOFS CJ I:/Thomas Telford/Sc/sc-39.3d Page: 8 SC 39 Keyword

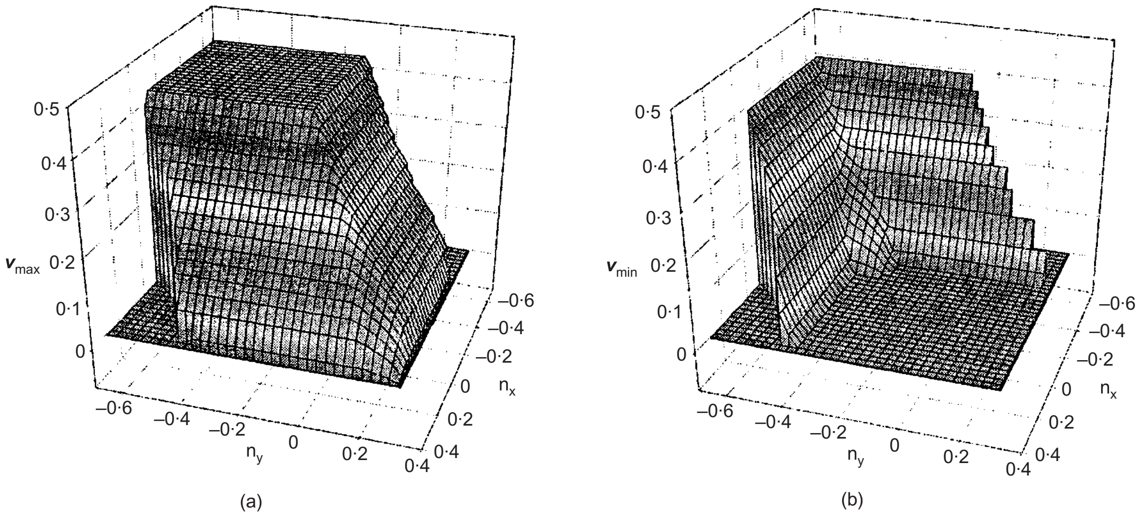

Fig. 10 Resisting domain for (a) $\boldsymbol{v}_{max}$ and (b) $\boldsymbol{v}_{min}$, where $\theta_{e1} = 45°$, $\omega_x = \omega_y = 0{\cdot}3$

$n_x = n_y = -0{\cdot}17/\vartheta_{el} = 45°$. It should noted that the presence of limit shear, $\boldsymbol{v}_{min}$, arising from the mathematical formulation of the model, identifies a situation in which failure of the reinforcement occurs by yielding in compression in pre-cracked elements.

This situation is very seldom encountered in actual fact, as it corresponds to non-monotonic loading conditions (not covered by the model) or at all events non-proportionally increasing conditions. In situations of this sort, in fact, a pre-cracked element might happen to have at least one order of reinforcement yielded in compression. This type of loading conditions is not covered by the proposed model, since it would be necessary to consider again the contribution of previously cracked concrete, which, upon the closing of the crack, recovers its ability to transfer compressive stresses normal to the crack. It is also possible to plot interaction surfaces $n_x/n_y/\boldsymbol{v}_{max}$ and $n_x/n_y/\boldsymbol{v}_{min}$ (Figures 10(a) and 10(b)) so as to achieve a presentation of the results formally similar to that of the Marti–Kaufmann model.

The resisting model for concrete described above can be refined further by making 6, non-dimensional with respect to $\boldsymbol{f}_{c2} = 0{\cdot}6(1 - \boldsymbol{f}_{ck}/250)|\boldsymbol{f}'_c|$, as defined in CEB-FIP Model Code 90, instead of $\boldsymbol{f}_c$; in this case, equation (63) can be replaced with a linear equation

$$\frac{\boldsymbol{\sigma}_c}{\boldsymbol{f}_{c2}} = 1 - 0{\cdot}032|\Delta\vartheta| \tag{74}$$

However, if the application of equation (74) supplies an estimate of the failure load for which no order of reinforcement turns out to be yielded, the calculation can be refined even further by repeating the computation by means of a corrected criterion, through the equation

$$\frac{\boldsymbol{\sigma}_c}{\boldsymbol{f}_{c2}} = 0{\cdot}85\frac{|\boldsymbol{f}'_c|}{\boldsymbol{f}_{c2}} - \frac{\boldsymbol{\sigma}_s}{\boldsymbol{f}_{ys}}\left(0{\cdot}85\frac{|\boldsymbol{f}'_c|}{\boldsymbol{f}_{c2}} - 1\right) \tag{75}$$

and iterating the process until two successive steps give two values of the ultimate load which are coincident for design purposes.

Comparison of the design models

From the foregoing considerations it can be seen that the only models that lend themselves to current design use (e.g. following a finite-element elastic-linear analysis) are the Marti–Kaufmann and the Carbone–Giordano–Mancini models.

Although both models make it possible to plot interaction surfaces, a direct comparison cannot be easily performed. It proves much easier to assess the degree of accuracy achieved by the two models in predicting a large number of test results which are generally deemed reliable.

This has been done by referring to the tests listed in Table 1.

The main mechanical parameters of these tests are reported in Table 2. In Table 3 the experimental (τ_{exp}) and calculated (τ_{cal}) maximum tangential stresses and the τ_{exp}/τ_{cal} related ratios are reported, following the Marti–Kaufmann and Carbone–Giordano–Mancini approaches.

In Figures 11(a) and 11(b) the same comparison between theoretical and experimental results is pictured. We can draw the following conclusions.

- The two models supply virtually identical results when failure is reached though the yielding of both orders of reinforcement.
- The Marti–Kaufmann model provides a better approximation in the presence of shear alone, but gives rise to appreciable errors in the presence of membrane actions and shear; in the latter case, in fact, it is exceedingly conservative.
- Although it is less accurate in the presence of shear alone, the Carbone–Giordano–Mancini model supplies the same degree of approximation even in the presence of shear and membrane actions.

Hence it can be concluded that for the design of RC membrane elements subjected to membrane actions and shear the second model is in closer agreement with physical reality.

Table 1 List of tests

Author	Test
Vecchio and Collins[3]	PV3/PV4/PV6/PV10/PV11/ PV12/PV16/ PV19/PV20/PV21/PV22/PV23/PV25/ PV27/PV28
Belarbi and Hsu[7]	A1/A2/A3/A4/B1/B2/B3/B4/B5/B6
Sumi and Kawamata[21]	A-1/A-2/A-3
Watanabe and Muguruma[22]	PL45D/PL45D1/PL45D2

FIRST PROOFS CJ I:/Thomas Telford/Sc/sc-39.3d Page: 9 SC 39 Keyword

Table 2 Mechanical parameters of tests

Test	σ_x/τ	σ_y/τ	ρ_x	f_{ysx} (MPa)	ρ_y	f_{ysy} (MPa)	f_c (MPa)
PV3	0·00	0·00	0·0048	662·0	0·0048	662·0	26·6
PV4	0·00	0·00	0·0106	242·0	0·0106	242·0	26·6
PV6	0·00	0·00	0·0179	266·0	0·0179	266·0	29·8
PV10	0·00	0·00	0·0179	276·0	0·0100	276·0	14·5
PV11	0·00	0·00	0·0179	235·0	0·0131	235·0	15·6
PV12	0·00	0·00	0·0179	469·0	0·0045	269·0	16·0
PV16	0·00	0·00	0·0074	255·0	0·0074	255·0	21·7
PV19	0·00	0·00	0·0179	458·0	0·0071	299·0	19·0
PV20	0·00	0·00	0·0179	460·0	0·0089	297·0	19·6
PV21	0·00	0·00	0·0179	458·0	0·0130	302·0	19·5
PV22	0·00	0·00	0·0179	458·0	0·0152	420·0	19·6
PV23	−0·39	−0·39	0·0179	518·0	0·0179	518·0	20·5
PV25	−0·69	−0·69	0·0179	466·0	0·0179	466·0	19·2
PV27	0·00	0·00	0·0179	442·0	0·0179	442·0	20·5
PV28	0·32	0·32	0·0179	483·0	0·0179	483·0	19·0
A1	0·00	0·00	0·00596	444·9	0·00596	444·9	42·2
A2	0·00	0·00	0·01193	462·8	0·01193	462·8	41·3
A3	0·00	0·00	0·01789	446·5	0·01789	446·6	41·7
A4	0·00	0·00	0·02982	469·9	0·02982	469·9	42·5
B1	0·00	0·00	0·01193	462·8	0·00596	444·9	45·3
B2	0·00	0·00	0·01789	446·6	0·01193	462·8	44·1
B3	0·00	0·00	0·01789	446·5	0·00596	444·9	44·9
B4	0·00	0·00	0·02982	469·9	0·00596	444·9	44·8
B5	0·00	0·00	0·02982	469·9	0·01193	462·8	42·8
B6	0·00	0·00	0·02982	469·9	0·01789	446·6	43·0
A-1	0·00	0·00	0·01060	400·0	0·01060	400·0	22·6
A-2	0·00	0·00	0·01470	400·0	0·01470	400·0	21·7
A-3	0·00	0·00	0·02000	400·0	0·02000	400·0	21·1
PL45D	0·00	0·00	0·00870	318·0	0·00870	318·0	28·1
PL45D1	0·00	0·00	0·01310	318·0	0·01310	318·0	30·9
PL45D2	0·00	0·00	0·02610	318·0	0·02610	318·0	30·9

Table 3 Experimental and calculated maximum tangential stresses

		Marti–Kaufmann		Carbone–Giordano–Mancini	
Test	τ_{exp} (MPa)	τ_{cal} (MPa)	τ_{exp}/τ_{cal}	τ_{cal} (MPa)	τ_{exp}/τ_{cal}
PV3	3·07	3·18	0·97	3·18	0·97
PV4	2·89	2·57	1·13	2·57	1·13
PV6	4·55	4·76	0·96	4·76	0·96
PV10	3·97	3·95	1·00	3·46	1·15
PV11	3·56	3·60	0·99	3·55	1·00
PV12	3·13	2·52	1·24	2·09	1·50
PV16	2·14	1·89	1·13	1·89	1·13
PV19	3·95	3·71	1·06	3·19	1·24
PV20	4·26	4·24	1·00	3·70	1·15
PV21	5·03	5·20	0·97	4·65	1·08
PV22	6·07	6·27	0·97	6·02	1·01
PV23	8·87	6·46	1·37	8·21	1·08
PV25	9·12	6·18	1·48	8·51	1·07
PV27	6·35	6·46	0·98	6·58	0·97
PV28	5·80	6·14	0·94	6·46	0·90
A1	2·28	2·65	0·86	2·65	0·86
A2	5·38	5·52	0·97	5·52	0·97
A3	7·67	7·99	0·96	7·99	0·96
A4	11·33	10·50	1·08	12·20	0·93
B1	3·97	3·83	1·04	3·77	1·05
B2	6·14	6·64	0·92	6·47	0·95
B3	4·37	4·60	0·95	4·77	0·92
B4	5·06	5·33	0·95	4·95	1·02
B5	7·17	8·02	0·89	7·61	0·94
B6	9·15	9·55	0·96	9·51	0·96
A-1	4·54	4·24	1·07	4·24	1·07
A-2	5·74	5·88	0·98	5·88	0·98
A-3	7·14	6·58	1·08	6·70	1·07
PL45D	2·84	2·77	1·03	2·77	1·03
PL45D1	3·97	4·17	0·95	4·17	0·95
PL45D2	7·60	8·49	0·90	8·30	0·92

Conclusions

In this study, several models for the design and checking of RC membrane elements are analysed and discussed with a view to identifying those that are in closest agreement with the experimental results. It is pointed out that only two models are suitable for practical design purposes, especially for the design and checking of elements designed using the finite-element method. While both models ensure acceptable degrees of reliability, the Marti–Kaufmann model yields more accurate results in dealing with elements subjected to shear alone, and the Carbone–Giordano–Mancini model is more suitable to deal with the simultaneous presence of all membrane actions.

Fig. 11 Experimental plotted against calculated panel strength by: (a) Marti and Kaufmann; and (b) Carbone, Giordano and Mancini

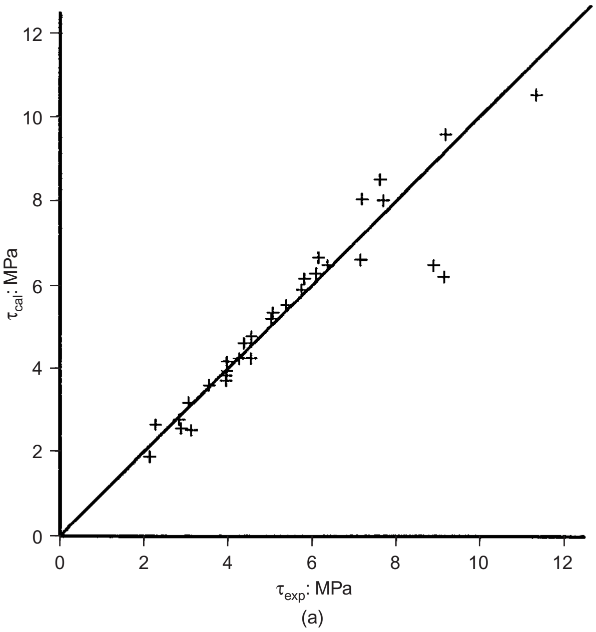

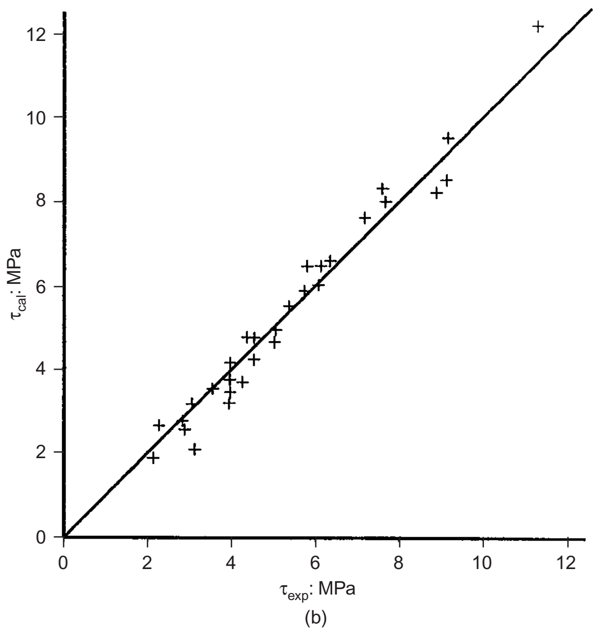

FIRST PROOFS CJ I:/Thomas Telford/Sc/sc-39.3d Page: 10 SC 39 Keyword

References

1. Collins, M. P. Stress–strain characteristics of diagonally cracked concrete. *Proceedings of a Colloquium on Plasticity in Reinforced Concrete*, Copenhagen, IABSE, 1979.
2. Vecchio, F. J. and Collins, M. P. Stress–Strain characteristics of reinforced concrete in pure shear. *Proceedings of a Colloquium on the Advanced Mechanism of Reinforced Concrete*, Delft, IABSE, 1981.
3. Vecchio, F. J. and Collins, M. P. *Response of Reinforced Concrete to In-plane Shear and Normal Stresses*. Department of Civil Engineering, University of Toronto, March 1982, Publication N. 82-03.
4. Vecchio, F. J. and Collins, M. P. The modified compression field theory for reinforced concrete elements subjected to shear. *ACI Journal*, 1986, March–April.
5. Hsu, T. T. C. Non linear analysis of concrete membrane elements. *ACI Journal*, 1991, September–October.
6. Belarbi, A. and Hsu, T. T. C. Constitutive laws of concrete in tension and reinforcing bars stiffened by concrete. *ACI Structural Journal*, 1994, July–August.
7. Belarbi, A. and Hsu, T. T. C. Constitutive laws of softened concrete in biaxial tension-compression. *ACI Structural Journal*, 1995, September–October.
8. Pang, X. B. and Hsu, T. T. C. Behaviour of reinforced concrete membrane elements in shear. *ACI Structural Journal*, 1995, November–December.
9. Pang, X. B. and Hsu, T. T. C. Fixed angle-softened-truss model for reinforced concrete. *ACI Structural Journal*, 1996, March–April.
10. Hsu, T. T. C. and Zang, L. X. Non linear analysis of membrane elements by fixed-angle softened-truss model. *ACI Structural Journal*, 1997, September–October.
11. Marti, P., Alvarez, M., Kaufmann, W. and Sigrist, V. Tension chord model for structural concrete. *Structural Engineering International*, 1998, No. 4/98.
12. Kaufmann, W. and Marti, P. Structural concrete: cracked membrane model. *Journal of Structural Engineering, ASCE*, 1998, December.
13. Kaufmann, W. Analysis of RC membranes in design practice. *Proceedings of a FIB Symposium*, Prague, September 1999.
14. Giordano, L. *Modelli Resistenti per Elementi Membranali in Calcestruzzo Armato e Precompresso*. Dissertation for doctoral degree in Structural Engineering, 12th Cycle, November 1999.
15. Carbone, V. I., Giordano, L. and Mancini, G. Design criterion for reinforced concrete panels subjected to in-plane forces. *Accademia delle Scienze di Torino, Atti Scienze Fisiche*, 1999, No. 133.
16. Carbone, V.I., Giordano, L. and Mancini, G., Resisting model for R.C. and P.C. panels. *Accademia delle Scienze di Torino, Atti Scienze Fisiche*, 2000, No. 134.
17. Walraven, J. C. Fundamental analysis of aggregate interlock. *Proceedings of ASCE*, 1981, **107**, No. ST11, November.
18. Baumann, T. Zur Frage der Netzbewehrung von Flächentragwerken. *Bauingenieur*, 1972, **47**, No. 10.
19. Von Grabe, W. and Tworuschka, H. An interface algorithm for non linear reliability analysis of reinforced concrete structures using ADINA. *Computer of Structures*, 1997, **64**, No. 5/6.
20. Kotsovos, M. D. A mathematical description of the strength properties of concrete under generalised stress. *Magazine of Concrete Research*, 1979, 151–158.
21. Sumi, K., Osa, M. and Kawamata, S. The governing factors of post cracking behaviour of reinforced concrete wall in in-plane shear. *The International Journal of Structural Mechanics and Materials Science*, Elsevier Applied Science, 1990, **29**, No. 3.
22. Watanabe, F. and Muguruma, H. Ultimate strength and deformation of RC panels. Structural design, analysis and testing. *Proceedings of Structure Congress '89, ASCE*, 1989.

V. I. Carbone
Politecnico of Turin, Italy

L. Giordano
Politecnico of Turin, Italy

G. Mancini
Politecnico of Turin, Italy